JACS
JOURNAL OF THE AMERICAN CHEMICAL SOCIETY
Article
pubs.acs.org/JACS

Water–Ice Analogues of Polycyclic Aromatic Hydrocarbons: Water Nanoclusters on Cu(111)

Melissa L. Liriano,[†] Chiara Gattinoni,[‡] Emily A. Lewis,[†] Colin J. Murphy,[†,§] E. Charles H. Sykes,[†] and Angelos Michaelides*[,‡]

[†]Department of Chemistry, Tufts University, Medford, Massachusetts 02155, United States
[‡]Thomas Young Centre, Department of Physics and Astronomy, London Centre for Nanotechnology, University College London, Gower Street, London WC1E 6BT, U.K.
[§]Competence Centre for Catalysis, Chalmers University of Technology, SE-412 96 Gothenburg, Sweden

Supporting Information

ABSTRACT: Water has an incredible ability to form a rich variety of structures, with 16 bulk ice phases identified, for example, as well as numerous distinct structures for water at interfaces or under confinement. Many of these structures are built from hexagonal motifs of water molecules, and indeed, for water on metal surfaces, individual hexamers of just six water molecules have been observed. Here, we report the results of low-temperature scanning tunneling microscopy experiments and density functional theory calculations which reveal a host of new structures for water–ice nanoclusters when adsorbed on an atomically flat Cu surface. The H-bonding networks within the nanoclusters resemble the resonance structures of polycyclic aromatic hydrocarbons, and water–ice analogues of inene, naphthalene, phenalene, anthracene, phenanthrene, and triphenylene have been observed. The specific structures identified and the H-bonding patterns within them reveal new insight about water on metals that allows us to refine the so-called "2D ice rules", which have so far proved useful in understanding water–ice structures at solid surfaces.

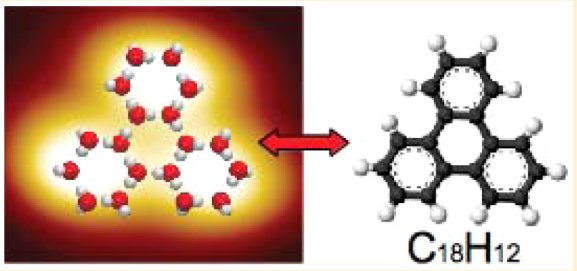

INTRODUCTION

Under ambient conditions, almost all solid surfaces are covered in a thin film of water.[1] The ubiquitous nature of water–solid interfaces means that they are relevant to an almost endless list of everyday and technological phenomena, ranging from the slipperiness of ice to electrochemical reactions and from ice formation to water purification. As a result of this widespread importance and the pressing need for clean water, renewable energy, and deeper insight into environmental chemical processes, interfacial water has been the subject of much detailed investigation. Great strides have been made in rationalizing water at interfaces from various perspectives, and the "field" of interfacial water is now flourishing.[2−9]

One area that has been particularly instrumental in improving understanding of interfacial water is the study of water on clean well-defined solid surfaces under ultrahigh vacuum conditions.[2,3,7,10] In these studies, the full arsenal of surface science techniques has been applied to interrogate interfacial water and obtain clear atomic and molecular-level insight. This has shed light on the chemistry of interfacial water and, in turn, on the balance between water–water and water–substrate bonding, precise information that is otherwise rarely available. Of the various techniques employed, the application of low-temperature scanning tunneling microscopy (LT-STM) has been particularly fruitful as it provides direct real-space images of the structures that water forms on surfaces.[6,10,11] When used in conjunction with density functional theory (DFT), this has exposed an incredible richness in the structures water can form at the surfaces of materials at low temperatures. On metal surfaces, for example, not only have structures comprising water hexamers (the building block of ice I) been identified,[12−21] but various other structures have been reported comprising pentamers,[22] heptamers, and combinations thereof.[23,24] Some of these structures are built exclusively from intact (non-dissociated) water molecules, whereas others contain mixtures of intact water molecules and hydroxyl groups, sometimes with highly defective H-bonding networks.[15,19,25] This body of work, along with earlier studies,[2] has been used to develop a set of so-called "2D ice rules",[10] which have been successfully used to rationalize how water bonds to certain metal surfaces (notably Pd and Ru) at low temperatures. These rules serve as an important complement to the traditional Bernal–Fowler–Pauling[26,27] ice rules for 3D bulk ice, which do not go far enough to explain water–ice structures at the interfaces of materials. However, the paucity of data means that it is unclear how far such rules can be extended. Understanding these structures is not just of fundamental interest, but it is an important first step in the rational design of substrates with

Received: February 22, 2017
Published: April 18, 2017

DOI: 10.1021/jacs.7b01883
J. Am. Chem. Soc. 2017, 139, 6403−6410

specific functionality, for example, for the control of ice formation, the flow of water, or water oxidation.

With this in mind, we report measurements on the adsorption and clustering of water at low coverages on Cu(111). Cu(111) has been a widely studied model system for water–ice adsorption,[28−34] in part because of its relevance to (electro)-catalysis and corrosion but also because water molecules remain intact on this surface (i.e., they do not dissociate) even under 0.1 Torr of H_2O pressure.[34,35] This, therefore, makes it possible to probe the interplay of water–water versus water–substrate interactions without the complications of hydroxyl group formation. Water coverage, sample preparation, and imaging conditions were similar to previously reported experimental settings,[30] except for a higher annealing temperature used in the present work. Indeed, this higher annealing temperature of 25 K (compared to 17 K[30]) is crucial in that it leads to the formation of large ordered clusters which have not been characterized before. These clusters (shown in Figure 1) appear in STM images as bi- or trilobed entities,

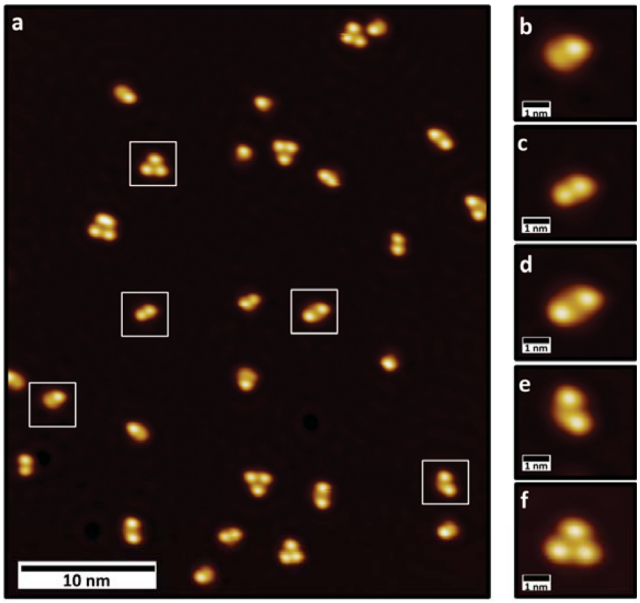

Figure 1. High-resolution STM images of submonolayer coverage of water on Cu(111) acquired at 5 K. Insets are zoomed-in images showing the five most prevalent ordered water clusters observed. (a) Large-area image of water clusters that form on Cu(111) after a 25 K anneal. (b) Water cluster referred to as the asymmetric dimer. (c) Smallest of the three bilobed features, referred to as the symmetric dimer. (d) Bilobed structure referred to as the long dimer. (e) Another bilobed water cluster referred to as the bent dimer. (f) Water trilobed structure. Scan conditions: +50 mV, 50 pA.

which with the help of DFT are shown to consist of interconnected hexamers and pentamers. Interestingly, we find that the oxygen skeletons of the structures identified resemble the carbon skeletons of polycyclic aromatic hydrocarbons (PAHs), and water superstructures corresponding to inene, naphthalene, phenalene, anthracene, phenanthrene, and triphenylene have been observed. In addition, the H-bonding networks suggested also bear some resemblance to the resonance structures of PAHs predicted by Clar's rules.[36] Current models for 2D ice growth are not fully compatible with the water nanoclusters identified here, and so in rationalizing these structures, we revise the existing 2D ice rules,[10] in a manner that we hope makes them more generally applicable.

In what follows, we first report details of the experimental and simulation setup. We then present structural models for the new water clusters identified in this study, followed by a discussion including a new set of 2D ice rules. Finally, conclusions and implications are presented.

METHODOLOGY

STM Experiments. All STM experiments were performed with an Omicron NanoTechnology low-temperature scanning tunneling microscope. To clean the Cu(111) single crystal, the sample was cleaned in a separate preparation chamber by sputtering with Ar^+ for two cycles (14 μA, 1 kV) and annealing (1000 K). The sample was then transferred to a precooled STM stage with a base temperature of 5 K and base pressure of 1×10^{-11} mbar or lower. Deionized water was obtained from a Nanopure water system and was further purified by first boiling the water (to reduce the amount of dissolved gas in the liquid) and then proceeding with freeze–pump–thaw cycles. Low coverages of water were deposited through a high-precision leak valve onto the surface held at 5 K followed by a thermal anneal to 25 K, which enabled the self-assembly of ordered clusters. The sample was then cooled back down to 5 K to acquire high-resolution images. STM images were obtained with Omicron chemically etched W tips at bias voltages between ±10 and ±50 mV and tunneling currents between 50 and 100 pA.

DFT Simulations. DFT calculations were performed within the periodic supercell approach using the VASP code.[37−40] The optB86b-vdW functional[41] was used throughout for the optimization of the adsorbed structures and the simulation of the STM images. The optB86b-vdW functional is a revised version of the van der Waals (vdW) density functional of Dion et al.,[42] which has shown good agreement with experimental results in a variety of molecular adsorption systems.[43−47] Although not shown, several of the adsorption structures examined in this study have been computed with two other vdW-inclusive functionals (vdW-DF2[48] and the method of Tkatchenko–Scheffler[49] applied on top of the Perdew–Burke–Ernzerhof (PBE)[50] functional) finding qualitatively similar results in all three cases. For comparison, calculations on the same range of structures were also performed with PBE, which does not include vdW interactions. Core electrons were replaced by projector-augmented wave (PAW) potentials,[51] whereas the valence states were expanded in planewaves with a cutoff energy of 500 eV. Adsorption calculations of superstructures formed by 6–18 molecules were carried out for water on four-layer (8 × 8) slabs separated by ∼15 Å of vacuum. For one of the considered structures (the "long dimer"), a three-layer thick (9 × 9) Cu(111) slab was considered instead to minimize lateral interactions between the periodic images of the water cluster. Within such unit cells, the shortest water–water interactions between periodic replicas are always 7 Å or more. This is adequate for characterizing the structures of the clusters observed in experiment, although the absolute water coverage in our simulations is higher than the experimental coverage of 0.05 monolayer (ML). The metal atoms in the bottom layer were fixed to the bulk optB86b-vdW (or PBE) optimal positions ($a_{Cu}^{optB86b\text{-}vdW}$ = 3.623 Å, a_{Cu}^{PBE} = 3.636 Å), whereas all other atoms were allowed to relax. A Monkhorst–Pack k-point grid of (2 × 2 × 1) was used in all calculations. A dipole correction along the direction perpendicular to the metal surface was applied, and geometry optimizations were performed with a residual force threshold of 0.01 eV/Å. A stricter convergence criterion (0.005 eV/Å) produced no noticeable difference in the structures and adsorption energies. STM images were simulated using the Tersoff–Hamann approach,[52] with a voltage of −500 mV and at a height of ∼6.5 Å above the metal surface. Simulated images for different voltages and tip height show similar results, demonstrating that the conclusion does not depend on the choice of parameters (see Supporting Information). Adsorption energies per molecule, E_{ads}, were computed with a standard definition:

$$E_{ads} = (E_{water/Cu(111)} - E_{Cu(111)} - n \times E_{H_2O})/n$$

DOI: 10.1021/jacs.7b01883
J. Am. Chem. Soc. 2017, 139, 6403−6410

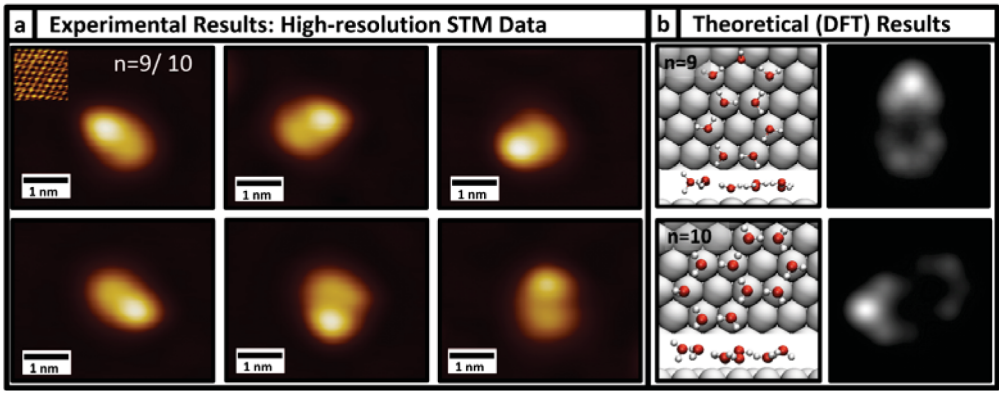

Figure 2. (a) High-resolution STM images, acquired at 5 K, of asymmetric dimers on Cu(111). An image of the underlying Cu(111) lattice is included (inset) to show the orientation of the symmetry axes of the Cu crystal used to perform all experiments. The asymmetric dimers are found in six different orientations and are aligned with the $\sqrt{3}$ direction of the underlying Cu surface. (b) Top panel is a DFT-calculated structure proposed for the asymmetric dimer, which is composed of nine water molecules (n = 9) arranged as a H-bonded pentamer and hexamer. The bottom panel shows an alternate and equally stable structure that consists of two H-bonded hexamers, composed of 10 water molecules (n = 10). The side views for both proposed structures show that water molecules common to both rings in each cluster lie flat on the surface while the outer portion of each ring is buckled. DFT-calculated STM images for each structure are shown on the far right, which match well with experimental results.

where the total energies of the n−water system, relaxed bare metal slab, and an isolated gas phase water molecule are, respectively, $E_{water/Cu(111)}$, $E_{Cu(111)}$, and E_{H_2O}. Favorable (exothermic) adsorption corresponds to negative values of the adsorption energy. It should be noted that adsorption energy differences between different H_2O/Cu(111) systems can be rather small, on the order of ∼15 meV. Therefore, to ensure that the quoted energy difference is meaningful, direct comparison of adsorption energies of different structures will be presented only for overlayer structures which have been optimized on the same slab and with the same parameters. The adsorption energy difference between the same structure optimized on the two different slabs was estimated to be 7 meV.

RESULTS

A low coverage of water (∼0.05 ML) was deposited on Cu(111), and LT-STM was used to image the pre-equilibrated sample. Mobile monomers, stable hexamers, and metastable aggregates were observed (see Figure S1), and these small water clusters match those previously reported for water on Cu(111) in ref 30. Moreover, a number of discrete, ordered clusters form at these conditions. and they are shown in Figure 1, with panel a showing a typical STM image of the surface after annealing to 25 K. The five most common cluster types are shown in panels b−f, and they exhibit either two or three bright lobes at subtly different distances and alignments with respect to the substrate. We will show in the following, through the combination of high-resolution STM data and DFT calculations, that several of the observed clusters have novel structures and resemble PAHs of ever-increasing size.

Asymmetric Dimer—9 or 10 Water Molecules. The first cluster that we discuss appears as a bilobed entity, with one lobe significantly brighter than the other. We therefore refer to this structure as an "asymmetric dimer"; the terminology here relates simply to the STM observation of two lobes and should not be confused with a dimer of two water molecules, which when imaged on metals is significantly smaller than the structures being discussed here.[4,21] The asymmetric dimer appeared in six different orientations, as shown in high-resolution STM images in Figure 2a, with the long axis of the cluster oriented in the $\sqrt{3}$ direction of Cu(111).

In order to arrive at plausible structural models for this adsorbed water aggregate, we performed an extensive set of DFT calculations. The configurational space for water clusters can be enormous even for moderate sizes. However, the large body of previous work for water on metals suggests that H-bonded structures built out of six- or five-membered water rings with most water molecules bonded directly above metal atoms of the substrate are most likely.[4,6,33] Indeed, from our DFT calculations, two low-energy structures (E_{ads} = −635 meV for both) of this type emerged as likely candidates for the experimentally observed cluster.

The first DFT-calculated structure consists of nine water molecules arranged in a double-looped configuration with a water hexamer H-bonded to a pentamer ring (top panel of Figure 2b). As expected, most molecules in this cluster both accept and donate H-bonds and are bonded directly above metal atoms of the substrate. There is one molecule, however, in the pentamer ring which is exclusively a H-bond acceptor. We refer to this water molecule which sits upright in the plane of the surface normal and accepts two H-bonds and donates none as a double acceptor (DA). Unlike the other water molecules, the DA is located above a hollow site of the substrate. The molecules in the cluster sit at different heights above the surface, with the lowest molecules at 2.15 Å and the highest-lying (DA) molecule at 3.20 Å. Ignoring this buckling for now and just considering the 2D projection of the oxygen "skeleton", this water cluster is an analogue of the carbon skeleton in the indene (C_9H_8) molecule. The simulated STM image of this nine-molecule cluster is shown in Figure 2b, and similar to the experimental image, it is bilobed with one lobe noticeably brighter than the other. The brighter contrast of one of the rings arises from the high-lying DA molecule in the pentamer ring. Indeed, we will see throughout that it is the presence of upright DA molecule in a ring that gives the ring a particularly bright contrast. As we will discuss below, simply by satisfying the existing 2D ice rules, DA molecules must always be present in structures containing more than one hexagonal or pentagonal ring. We note in passing that we have considered the possibility that the bright features in the STM simulations assigned here to DA water molecules might be OH groups. However, the agreement with the experimental STM image is significantly worse if a DA water molecule is replaced with an OH. In particular, OH images less brightly than water, mainly

DOI: 10.1021/jacs.7b01883
J. Am. Chem. Soc. 2017, 139, 6403−6410

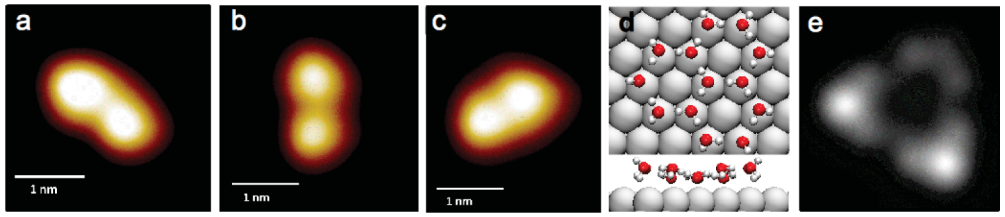

Figure 3. (a–c) High-resolution STM image of a bilobed feature, referred to as the symmetric dimer, in the three possible orientations. (d) DFT-calculated structure proposed for the symmetric dimer, which consists of 13 water molecules arranged as three interconnected H-bonded hexamers. (e) DFT-calculated STM image of the proposed n = 13 water cluster, which matches well with experimental data.

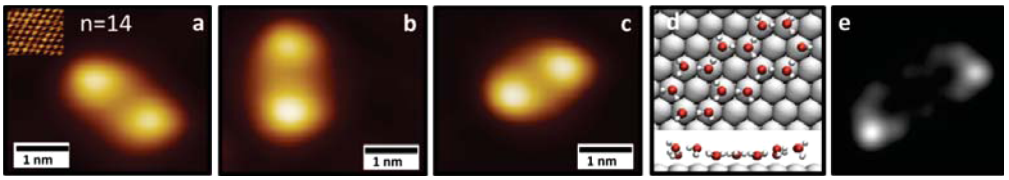

Figure 4. (a–c) High-resolution STM image, acquired at 5 K, of the bilobed structure referred to as the long dimer, which is found in three different orientations on the Cu surface. The inset is an atomic-scale image of the Cu(111) single-crystal substrate upon which the clusters are adsorbed. (d) DFT-calculated structure proposed for the experimentally observed long dimer, which is composed of three H-bonded water hexamers (14 water molecules) arranged in a linear configuration. The side view shows that the predicted structure consists of a central flat hexamer flanked by two buckled water hexamers. (e) DFT-simulated STM image of the proposed n = 14 water cluster, indicating that the DA water molecules image as two bright protrusions.

because it resides much closer to the surface than the water molecules. The absence of OH groups in the structures is consistent with earlier studies which show that water does not dissociate on Cu(111)[34,35] and the lack of any detectable hydrogen on our surface.

The second structure, which also agrees well with the size and rotational orientation measurements of the experimentally observed asymmetric dimer, consists of 10 water molecules on atop sites, arranged as two H-bonded water hexamers (Figure 2b, bottom panel). This superstructure is a water cluster analogue of naphthalene ($C_{10}H_8$). As with the nine-molecule cluster, this structure contains one DA molecule in one of the two rings, and it is the presence of this high-lying molecule (d_{O-Cu} = 3.21 Å) that creates the asymmetric contrast, as shown in the simulated STM image of this structure at the bottom of Figure 2b. Overall both nine- and 10-molecule structures offer a similar level of agreement with experiment, and they are equally plausible models for the observed clusters.

Before moving on to the larger structures, we note that, previously,[30] another n = 9 cluster, a water nonamer, was proposed. This water cluster comprises a central water hexamer with three additional molecules bonded at the periphery to every other molecule of the hexamer (see Figure S3 in the Supporting Information). Interestingly, in our study, the calculated n = 9 structure composed of a pentamer H-bonded to a hexamer is ever so slightly (16 meV) more stable than this previously reported water nonamer. When postulating the 2D ice rules to describe water growth on Pd(111) and Ru(0001) surfaces, we found that the most energetically stable clusters consisted of water molecules that were able to form as many H-bonds as possible.[10] This suggests that, in our study, the added stability found in the proposed n = 9 structure is due to the "closed-loop" because four additional H-bonds are formed (with respect to the hexamer), relative to the three H-bonds formed with under-coordinated water molecules in the nonamer. This preference for closed-loop structures also explains why binding to a hollow site is energetically favorable for the DA molecule in the pentameric loop of the n = 9 structure as binding to an atop site would result in an opened ring system with under-coordinated molecules that have unsatisfied H-bonds.

Symmetric Dimer—13 Water Molecules. The next nanocluster we discuss, shown in Figure 3, is imaged as two lobes of equal brightness. We refer to this structure as the "symmetric dimer". The DFT calculations show that an ordered cluster composed of three H-bonded water hexamers (Figure 3d), comprising 13 water molecules, is the most energetically stable cluster (with E_{ads} = −645 meV) that is consistent with the size and rotational orientation measurements of the observed symmetric bilobes in Figure 3a–c. This water cluster is analogous to the phenalene ($C_{13}H_{10}$) molecule. In Figure 3d, the side view of the proposed n = 13 water cluster shows that, while all water molecules sit on preferred atop sites, they have different O–Cu distances; two of the hexamer loops contain a DA molecule at the periphery of each ring, and each DA lies ∼3.2 Å above the surface. Also, consistent with predictions for the n = 13 structure, the DA-containing rings can be found in two of the three high-symmetry directions of the Cu surface, resulting in three possible orientations, all of which are experimentally observed (Figure 3a–c).

We note that this structure resembles the previously reported water octamer.[30] The distance separating the two lobes is comparable in the two structures (∼0.75 nm for the structure in Figure 3a–c and ∼0.81 nm for the octamer), but the present cluster shows an additional dimmer central lobe. In the current study, the most common bilobed feature is the proposed n = 13 structure, whereas the smaller octamer was less common. This is again consistent with the finding that closed-looped structures are energetically more stable and therefore more prevalent on this surface after annealing to 25 K.

Long Dimer—14 Water Molecules. In Figure 4a–c, our high-resolution STM images show another set of bilobed structures, referred to as "long dimers", which are found in three different orientations. While these dimers are oriented in the $\sqrt{3}$ direction of the underlying substrate, lateral size measurements show, however, that the average lobe–lobe

DOI: 10.1021/jacs.7b01883
J. Am. Chem. Soc. 2017, 139, 6403–6410

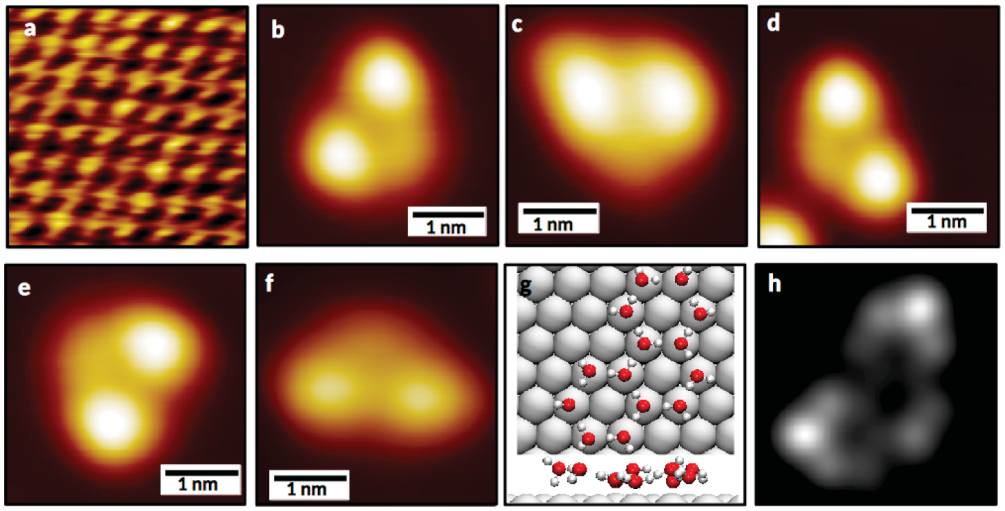

Figure 5. High-resolution STM images acquired at 5 K. (a) Atomic-scale image of the Cu(111) single crystal used to perform all experiments. (b–f) High-resolution STM image of the observed bilobe structure, with a dimmer central protrusion, referred to as the bent dimer. (g) DFT-calculated structure proposed for the bent dimer, which is an isomer of the DFT structure proposed for the long dimer in Figure 4, as it also consists of three interconnected hexamers, or 14 water molecules, but in a bent arrangement. The side view shows that the predicted configuration involves a central partially flat hexamer flanked by two buckled water hexamers. (h) DFT-simulated STM of the proposed n = 14 bent dimer, which matches well with experimental observations.

distance is 1.20 ± 0.08 nm, which is significantly longer than the distance measured for the symmetric (n = 13) dimer in Figure 3a–c. This suggests the presence of yet another type of water cluster. Indeed, DFT calculations reveal that the most stable cluster (with E_{ads} = −645 meV) that agrees with experimental size and rotation measurements consists of three connected hexamers (n = 14) arranged in a linear configuration, resembling the carbon analog anthracene ($C_{14}H_{10}$), as illustrated in Figure 4d. The central ring is not buckled, being composed solely of low-lying (d_{O-Cu} ∼ 2.30 Å) water molecules. In contrast, the outer rings contain one DA water molecule each and are further composed of low-lying (d_{O-Cu} ∼ 2.35 Å) and high-lying (d_{O-Cu} ∼ 3.05 Å) water molecules, all sitting on Cu atop sites. Similar to the n = 13 symmetric dimer, the n = 14 linear dimer images as two bright protrusions, with the brightness being attributed to the DA water molecules that are sitting the highest above the surface with an O–Cu distance of 3.20 Å. DFT calculations predict that the energetically preferred position of the DA water molecules is at the periphery of the ring structures, as illustrated in the side view of the DFT-calculated structure in Figure 4d. This prediction is consistent with experimental data as only bilobes with equal brightness at the ends of the structures have been imaged with STM.

Bent Dimer—14 Water Molecules. High-resolution images of the fourth set of observed bilobed structures, which we refer to as "bent dimers", are shown in Figure 5b–f. The average lobe–lobe distance is 1.11 ± 0.04 nm, and they have a central, dimmer region. The higher-lying features or the two brightest protrusions run almost parallel to the close-packed direction of the underlying Cu surface and exist in at least five different orientations. The proposed DFT structure for the bent dimer (Figure 5g, E_{ads} = −643 meV) is an isomer of the long dimer, as it is composed of 14 water molecules (n = 14), or three water hexamers, arranged in a bent formation. This is structurally comparable to the carbon-based compound phenanthrene ($C_{14}H_{10}$). As shown in Figure 5b–f, the bent dimers appear as two bright protrusions flanking a dimmer, lower-lying portion of the water adstructure. This is consistent with the DFT-predicted model of outer buckled rings containing one DA water molecule each (at d_{O-Cu} ∼ 3.22 Å), as well as alternating low-lying and high-lying molecules, all sitting higher above the Cu(111) surface than the water molecules in the partially flat central water hexamer (whose molecules are at d_{O-Cu} = 2.18 Å). Based on the bent structure predicted by DFT, and due to the three-fold symmetry of the Cu(111) surface, the bent dimer is expected to exist in three different configurations with each having an "up" and "down" orientation, resulting in a total of six clusters. Experimentally, we observe five, which is reasonable given Poisson statistics and the total area searched.

Trilobed Cluster—18 Water Molecules. The final cluster we report is the trilobed structure shown in Figure 6a. Once again, the STM image of this structure resembles a previously reported nine-water molecule trilobe structure;[30] however, further experimental measurements reveal major features indicating that these complexes are larger than the previously reported nonamer. The first observation is that there are two different types of trilobed features that exist in "up" and "down" orientations, resulting in four structures instead of the two expected for the water nonamer. This suggests that the rotational orientations for these trilobed features are due to actual rotations of the structure relative to the close-packed direction of the Cu(111) lattice and not the migration of monomeric units of water, as predicted and observed for the smaller water nonamers. The second observation is that the rotations of the trilobed structures are aligned almost parallel to the high-symmetry axis of the underlying surface and not with the $\sqrt{3}$ direction as predicted and observed for the water nonamer. Experimental measurements indicate that one type of trilobe structure is rotated +4° from the close-packed direction of the Cu(111) surface whereas the second is orientated −4°, making these structures chiral.

DFT calculations predict that the most stable cluster for this trilobed structure (with E_{ads} = −650 meV) is composed of four H-bonded hexamers, or 18 water molecules (n = 18), with three buckled hexamers arranged around a flat central water

DOI: 10.1021/jacs.7b01883
J. Am. Chem. Soc. 2017, 139, 6403–6410

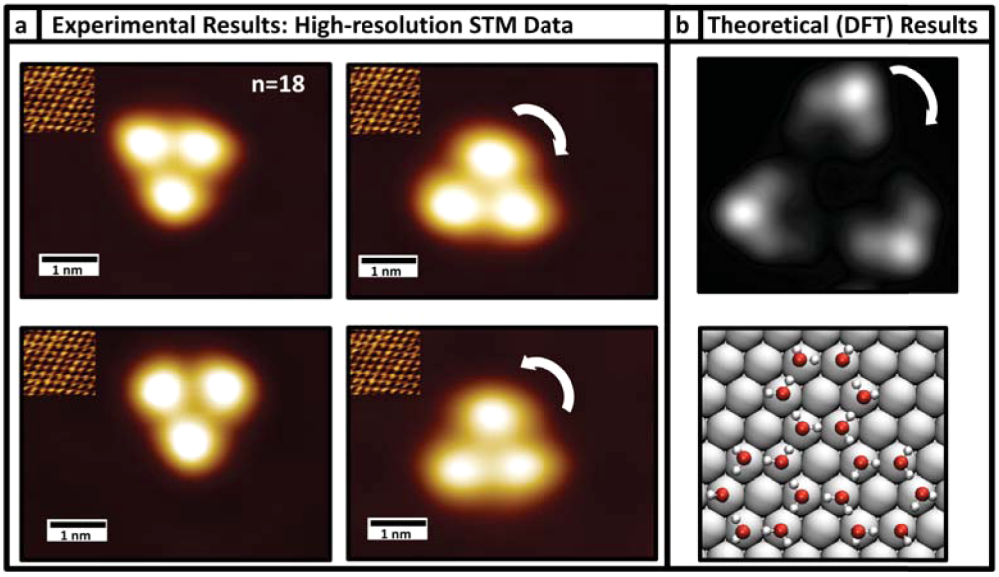

Figure 6. (a) High-resolution STM images acquired at 5 K of two chiral trilobed structures, with each chiral conformer found in an up and down orientation. (b) (Top) DFT-simulated image of the proposed trilobed structure, indicating that the three DA water molecules image as three bright protrusions. Because the positions of DA molecules can alternate within their respective hexamer rings, the trilobed clusters are chiral as they are rotated slightly from the high symmetry axes of the Cu(111) surface. (Bottom) DFT-calculated structure proposed for the trilobed structures, which consist of four H-bonded hexamers or of 18 water molecules.

hexamer (Figure 6b). This hexagonal arrangement is analogous to the organic compound triphenylene ($C_{18}H_{12}$). The DFT-calculated structure in Figure 6b shows that all water molecules sit on preferred atop sites, and each outer hexagonal ring contains one DA water molecule. As with all the other proposed structures, DFT calculations show that the O−Cu distance in the DA molecules is ∼3.20 Å, whereas the O atoms in the central flat hexamer lie much closer to the surface with O−Cu distances of ∼2.20 Å. The three bright lobes observed in the STM images and the lack of resolution of the central flat hexamer are consistent with this structural prediction. Furthermore, the highest-lying molecules, the DAs, can isoenergetically H-bond in two different positions at the periphery of their respective buckled hexamer, giving rise to conformational isomers of the structure. Experimentally, this is confirmed by observations of chiral trilobed structures.

We finally note that even more complex supramolecular water structures can be obtained at higher annealing temperatures. Indeed, we find that annealing to ∼40 K results in the formation of 3D water clusters, indicating that these supramolecular assemblies discussed here are metastable structures. This is consistent with earlier work.[53,54] We show some of these 3D structures in Figure S1, but these structures remain outside the scope of this work and will not be analyzed in detail.

■ DISCUSSION

Having identified a new set of structures for water nanoclusters on Cu, we now place these results in a somewhat broader context. The structures identified here for water clusters comprising 9−18 molecules differ significantly from gas phase water clusters in this size regime.[55] This difference arises from the interaction with the substrate, and we now look into this issue in more detail focusing, in particular, on the subtle balance of water−water and water−metal bonding. Following this, we discuss how the new structures identified and insight obtained relate to the so-called 2D ice rules.

To Buckle or Not To Buckle? The novel structures presented in this work are mostly formed of H-bonded water hexamers. Previous DFT calculations found that in isolated water hexamers on Cu(111), the constitutive molecules were at two distinct heights above the surface (i.e., the clusters were buckled). Specifically, every second molecule in the hexamer was ∼0.76 Å further from the surface than the other three molecules.[30,31] See also the Supporting Information for the structure of the buckled hexamer. The buckled configuration was explained in terms of the competition between H-bonding between adjacent H_2O molecules and H_2O−metal interactions. The two compete because the same orbital is involved in both accepting a H-bond and in bonding with the metal surface. In addition, it was shown that as one moved from Cu to more reactive metals such as Pd and Ru, the hexamers flattened because of the increased interaction strength of water with this substrates.[2,3,30,33] Consistent with the earlier work, we find that an isolated water hexamer on Cu(111) is indeed buckled with the distances from the surface being 2.35 and 3.30 Å. However, interestingly, we find that as the nanoclusters get larger, there is a tendency for their structure to flatten as the central or internal water molecules get closer to the surface. The hexamers in the center of the long dimer and the trilobed structure, for example, have flat central cores, with all molecules in the central hexamer of each ∼2.15 Å from the surface. In contrast, the hexamers on the periphery of these structures, which contain the high-lying DA molecules, are buckled. Detailed analysis of the various structures, including decompositions of the total adsorption energies into water−water and water−substrate contributions (available in the Supporting Information), reveals that the flattening arises from a weakening of the H-bonding network and a subsequent greater water−substrate bonding in the larger water clusters. Thus, we see here that in addition to altering the adsorbate−substrate interaction strength and subsequent adsorption structure upon moving from one metal to the next, simply by changing the size of the water nanocluster, the

DOI: 10.1021/jacs.7b01883
J. Am. Chem. Soc. 2017, 139, 6403−6410

interaction strength and structure of the water cluster is modified.

2D Ice Rules. The results presented so far highlight the complexity of ice formation on metal surfaces. Ice formation is shown, in this and previous studies, to be driven by the balance between intermolecular H-bonding and water−surface interactions. It is therefore influenced by the particular surface on which water is deposited. The 2D ice rules, formulated for submonolayer ice growth on Pd(111) and Ru(0001) below 130 K, have established that (i) H_2O molecules bind on atop sites of metal atoms through the oxygen lone pair in a flat orientation; (ii) H_2O molecules form as many H-bonds as possible; and (iii) H_2O cluster growth is terminated when condition (ii) cannot be satisfied, restricting the unsatisfied or nondonor bond to the periphery of the water cluster.[10] Whereas these established ice rules can be loosely applied to this system, they do not adequately explain all the structures observed. For example, our study reveals that the most stable nine-molecule structure on Cu(111) is a closed-ring system (Figure 2) containing a hexamer and a pentamer. This is in violation of rule (i) because one H_2O in the pentamer is not on an atop site, whereas all molecules in the nonamer of refs 30 and 31 are. It, however, satisfies rule (ii) as the closed-loop structure maximizes the number of H-bonds in the system. In addition the observation of buckled structures, most notably a buckled hexamer, is in violation of rule (i) because certain H_2O molecules in this structure do not bond in a flat orientation.

While recognizing the success of the 2D ice rules, upon slight revision, we find that they can be extended to structures identified here on Cu(111). We therefore propose the following reformulated rules:

(i) Water molecules preferentially form closed-loop structures comprising five or more water molecules. Expanding upon this, we further suggest that the water molecules within these loops preferentially donate and accept a single H-bond. At a "node" between two loops, double donor−single acceptor water molecules are expected. Structures containing single acceptors-zero donors are less stable.

(ii) Water molecules preferably bind to metal atoms at the atop position as long as that leads to the formation of closed-loop structures, that is, as long as rule (i) is followed.

(iii) There are as few double acceptors as possible in a superstructure. For finite clusters, this implies that there are $N - 1$ DAs (N being the number of closed loops). In the pentagonal linear chains that form on Cu(110),[22] there are N DAs, and in the lace-like structure on Pd,[19] there are $N + 1$ DAs.

(iv) For finite clusters, the DA molecules reside preferentially in closed loops at the periphery of a structure.

As a final comment, we note that our revised ice rules have an analogy with Clar's rule formulated in 1972 for predicting the aromatic character of PAHs.[36] Specifically, Clar's rule predicts that the most stable structure of PAHs has the maximum number of aromatic sextets, which cannot be neighbors, with the constraint that a Kekulé structure must be written for the rest of the PAH. Maximizing the number of non-neighboring sextets has the implication that these sextets are generally positioned at the periphery of the PAH structure (e.g., see structures in ref 56). Similarly, here, we see that the water nanoclusters that form on Cu(111) maximize the number of H-bonds, thus preferring looped structures and penalizing structures with single acceptors−zero donors. Moreover, DAs are found as far away from each other as possible, on non-neighboring hexamers, and therefore in the outer rings of the water clusters. The only exception here is the case of the symmetric dimer (composed of three neighboring rings) where two of the DAs are on adjacent rings because, otherwise, rule (iii) would be violated and there would be fewer than $N - 1$ DAs. Clar's rules have been employed to help interpret experimental results and characterize a large number of PAHs.[56] In the same way, the proposed ice rules can guide future research on clusters on metal substrates and help interpret experimental results. Whereas the shape of the cluster itself (e.g., whether it is formed of hexagons or pentagons, whether it is buckled or flat) will depend strongly on the strength of the water−substrate interaction and on the packing of the substrate, the interpretation of experimental results should favor structures with a H-bonding network compatible with the presently stated rules.

CONCLUSIONS

In this work, a number of new features for water nanocluster formation on Cu(111) have been predicted and observed, thereby providing a greater understanding of how ordered water structures form and grow on metal surfaces. A combination of LT-STM and DFT calculations was used to characterize a set of ordered water clusters that formed when a submonolayer concentration of water was deposited on a Cu surface, annealed to ∼25 K, and imaged at 5 K. We confirmed that ice nucleation commences with the formation of a stable buckled water hexamer, and further cluster growth is stabilized by the "flattening" of the central portion of the superstructure. The desire to maximize the number of H-bonds is a key characteristic of the structures observed; on this particular surface, closed-loop structures, with interconnected rings H-bonded via flat, low-lying molecules, are more stable than opened-ring systems. Furthermore, molecules will deviate from preferred atop binding sites in order to form the more stable closed-ring structures. Based on these findings, we have proposed a set of new conditions that expand on the existing 2D ice rules[10] for submonolayer coverages of water. These rules still describe ice growth on other metal surfaces while accounting for the emergence and stability of these larger, ordered water clusters observed on Cu(111).

ASSOCIATED CONTENT

Supporting Information

The Supporting Information is available free of charge on the ACS Publications website at DOI: 10.1021/jacs.7b01883.

Additional STM figures and DFT analysis (PDF)

AUTHOR INFORMATION

Corresponding Author

*angelos.michaelides@ucl.ac.uk

ORCID

Chiara Gattinoni: 0000-0002-3376-6374

E. Charles H. Sykes: 0000-0002-0224-2084

Angelos Michaelides: 0000-0002-9169-169X

Notes

The authors declare no competing financial interest.

ACKNOWLEDGMENTS

Work at UCL was supported by the European Research Council under the European Union's Seventh Framework

DOI: 10.1021/jacs.7b01883
J. Am. Chem. Soc. 2017, 139, 6403−6410

Programme (FP/2007-2013)/ERC Grant Agreement No. 616121 (HeteroIce project). A.M. is also supported by the Royal Society through a Royal Society Wolfson Research Merit Award. We are grateful to the London Centre for Nanotechnology for computational resources, UCL Research Computing, and to the UKCP consortium (Grant No. EP/F036884/1) for access to Archer. The work at Tufts University was supported by the Department of Energy BES under Grant No. DE-SC0008703. M.L.L. thanks the NSF for a Graduate Research Fellowship.

REFERENCES

(1) Ewing, G. E. *Chem. Rev.* **2006**, *106*, 1511.
(2) Thiel, P. A.; Madey, T. E. *Surf. Sci. Rep.* **1987**, *7*, 211.
(3) Henderson, M. A. *Surf. Sci. Rep.* **2002**, *46*, 1.
(4) Maier, S.; Salmeron, M. *Acc. Chem. Res.* **2015**, *48*, 2783.
(5) Björneholm, O.; Hansen, M. H.; Hodgson, A.; Liu, L.-M.; Limmer, D. T.; Michaelides, A.; Pedevilla, P.; Rossmeisl, J.; Shen, H.; Tocci, G.; Tyrode, E.; Walz, M.-M.; Werner, J.; Bluhm, H. *Chem. Rev.* **2016**, *116*, 7698.
(6) Carrasco, J.; Hodgson, A.; Michaelides, A. *Nat. Mater.* **2012**, *11*, 667.
(7) Hodgson, A.; Haq, S. *Surf. Sci. Rep.* **2009**, *64*, 381.
(8) Striolo, A. *Adsorpt. Sci. Technol.* **2011**, *29*, 211.
(9) Verdaguer, A.; Sacha, G. M.; Bluhm, H.; Salmeron, M. *Chem. Rev.* **2006**, *106*, 1478.
(10) Salmeron, M.; Bluhm, H.; Tatarkhanov, M.; Ketteler, G.; Shimizu, T. K.; Mugarza, A.; Deng, X.; Herranz, T.; Yamamoto, S.; Nilsson, A. *Faraday Discuss.* **2009**, *141*, 221.
(11) Guo, J.; Bian, K.; Lin, Z.; Jiang, Y. *J. Chem. Phys.* **2016**, *145*, 160901.
(12) Maier, S.; Stass, I.; Mitsui, T.; Feibelman, P. J.; Thürmer, K.; Salmeron, M. *Phys. Rev. B: Condens. Matter Mater. Phys.* **2012**, *85*, 155434.
(13) Massey, A.; McBride, F.; Darling, G. R.; Nakamura, M.; Hodgson, A. *Phys. Chem. Chem. Phys.* **2014**, *16*, 24018.
(14) McBride, F.; Omer, A.; Clay, C. M.; Cummings, L.; Darling, G. R.; Hodgson, A. *J. Phys.: Condens. Matter* **2012**, *24*, 124102.
(15) Forster, M.; Raval, R.; Hodgson, A.; Carrasco, J.; Michaelides, A. *Phys. Rev. Lett.* **2011**, *106*, 046103.
(16) Gallagher, M.; Omer, A.; Darling, G. R.; Hodgson, A. *Faraday Discuss.* **2009**, *141*, 231.
(17) Morgenstern, K. *Surf. Sci.* **2002**, *504*, 293.
(18) Tatarkhanov, M.; Ogletree, D. F.; Rose, F.; Mitsui, T.; Fomin, E.; Maier, S.; Rose, M.; Cerdá, J. I.; Salmeron, M. *J. Am. Chem. Soc.* **2009**, *131*, 18425.
(19) Cerdá, J. I.; Michaelides, A.; Bocquet, M. L.; Feibelman, P. J.; Mitsui, T.; Rose, M.; Fomin, E.; Salmeron, M. *Phys. Rev. Lett.* **2004**, *93*, 116101.
(20) Feibelman, P. J. *Science* **2002**, *295*, 99.
(21) Ogasawara, H.; Yoshinobu, J.; Kawai, M. *J. Chem. Phys.* **1999**, *111*, 7003.
(22) Carrasco, J.; Michaelides, A.; Forster, M.; Haq, S.; Raval, R.; Hodgson, A. *Nat. Mater.* **2009**, *8*, 427.
(23) Maier, S.; Lechner, B. A. J.; Somorjai, G. A.; Salmeron, M. *J. Am. Chem. Soc.* **2016**, *138*, 3145−3151.
(24) Nie, S.; Feibelman, P. J.; Bartelt, N. C.; Thürmer, K. *Phys. Rev. Lett.* **2010**, *105*, 026102.
(25) Tatarkhanov, M.; Fomin, E.; Salmeron, M.; Andersson, K.; Ogasawara, H.; Pettersson, L. G. M.; Nilsson, A.; Cerdá, J. I. *J. Chem. Phys.* **2008**, *129*, 154109.
(26) Bernal, J. D.; Fowler, R. H. *J. Chem. Phys.* **1933**, *1*, 515.
(27) Pauling, L. *J. Am. Chem. Soc.* **1935**, *57*, 2680.
(28) Morgenstern, K.; Gawronski, H.; Mehlhorn, M.; Rieder, K.-H. *J. Mod. Opt.* **2004**, *51*, 2813.
(29) Mehlhorn, M.; Carrasco, J.; Michaelides, A.; Morgenstern, K. *Phys. Rev. Lett.* **2009**, *103*, 026101.
(30) Michaelides, A.; Morgenstern, K. *Nat. Mater.* **2007**, *6*, 597.
(31) Michaelides, A. *Faraday Discuss.* **2007**, *136*, 287.
(32) Morgenstern, K.; Rieder, K.-H. *J. Chem. Phys.* **2002**, *116*, 5746.
(33) Michaelides, A.; Ranea, V. A.; de Andres, P. L.; King, D. A. *Phys. Rev. Lett.* **2003**, *90*, 216102.
(34) Yamamoto, S.; Bluhm, H.; Andersson, K.; Ketteler, G.; Ogasawara, H.; Salmeron, M.; Nilsson, A. *J. Phys.: Condens. Matter* **2008**, *20*, 184025.
(35) Eren, B.; Zherebetskyy, D.; Patera, L. L.; Wu, C. H.; Bluhm, H.; Africh, C.; Wang, L.-W.; Somorjai, G. A.; Salmeron, M. *Science* **2016**, *351*, 475.
(36) Clar, E. *the Aromatic Sextet*; Wiley: London, 1972.
(37) Kresse, G.; Hafner, J. *Phys. Rev. B: Condens. Matter Mater. Phys.* **1993**, *47*, 558.
(38) Kresse, G.; Hafner, J. *Phys. Rev. B: Condens. Matter Mater. Phys.* **1994**, *49*, 14251.
(39) Kresse, G.; Furthmueller, J. *Comput. Mater. Sci.* **1996**, *6*, 15.
(40) Kresse, G.; Furthmueller, J. *Phys. Rev. B: Condens. Matter Mater. Phys.* **1996**, *54*, 11169.
(41) Klimeš, J.; Bowler, D. R.; Michaelides, A. *Phys. Rev. B: Condens. Matter Mater. Phys.* **2011**, *83*, 195131.
(42) Dion, M.; Rydberg, H.; Schröder, E.; Langreth, D. C.; Lundqvist, B. I. *Phys. Rev. Lett.* **2004**, *92*, 246401.
(43) Lew, W.; Crowe, M. C.; Campbell, C. T.; Carrasco, J.; Michaelides, A. *J. Phys. Chem. C* **2011**, *115*, 23008.
(44) Murphy, C. J.; Carrasco, J.; Lawton, T. J.; Liriano, M. L.; Baber, A. E.; Lewis, E. A.; Michaelides, A.; Sykes, E. C. H. *J. Chem. Phys.* **2014**, *141*, 014701.
(45) Carrasco, J.; Liu, W.; Michaelides, A.; Tkatchenko, A. *J. Chem. Phys.* **2014**, *140*, 084704.
(46) Liu, W.; Carrasco, J.; Santra, B.; Michaelides, A.; Scheffler, M.; Tkatchenko, A. *Phys. Rev. B: Condens. Matter Mater. Phys.* **2012**, *86*, 245405.
(47) Gattinoni, C.; Michaelides, A. *Faraday Discuss.* **2015**, *180*, 439.
(48) Lee, K.; Murray, E. D.; Kong, L.; Lundqvist, B. I.; Langreth, D. C. *Phys. Rev. B: Condens. Matter Mater. Phys.* **2010**, *82*, 081101.
(49) Tkatchenko, A.; Scheffler, M. *Phys. Rev. Lett.* **2009**, *102*, 073005.
(50) Perdew, J. P.; Burke, K.; Ernzerhof, M. *Phys. Rev. Lett.* **1996**, *77*, 3865.
(51) Kresse, G.; Joubert, D. *Phys. Rev. B: Condens. Matter Mater. Phys.* **1999**, *59*, 1758.
(52) Tersoff, J.; Hamann, D. R. *Phys. Rev. B: Condens. Matter Mater. Phys.* **1985**, *31*, 805.
(53) Mehlhorn, M.; Morgenstern, K. *New J. Phys.* **2009**, *11*, 093015.
(54) Stähler, J.; Mehlhorn, M.; Bovensiepen, U.; Meyer, M.; Kusmierek, D. O.; Morgenstern, K.; Wolf, M. *Phys. Rev. Lett.* **2007**, *98*, 206105.
(55) Xantheas, S. S.; Dunning, T. H., Jr. *J. Chem. Phys.* **1993**, *99*, 8774.
(56) Solá, M. *Front. Chem.* **2013**, *1*, 22.

DOI: 10.1021/jacs.7b01883
J. Am. Chem. Soc. 2017, 139, 6403−6410